University of Wollongong
Research Online

Faculty of Informatics - Papers (Archive)

Faculty of Engineering and Information Sciences

2010

Quasi-orthogonal space-time-frequency codes in MB-OFDM UWB

Le Chung Tran
University of Wollongong, lctran@uow.edu.au

Alfred Mertins
University of Luebeck, Germany, mertins@isip.uni-luebeck.de

Tadeusz A. Wysocki
University of Nebraska - Lincoln, USA, twysocki@mail.unomaha.edu

Publication Details

L. Tran, A. Mertins & T. A. Wysocki, "Quasi-orthogonal space-time-frequency codes in MB-OFDM UWB," Computers & Electrical Engineering, vol. 36, (4) pp. 766-774, 2010.

Research Online is the open access institutional repository for the University of Wollongong. For further information contact the UOW Library: research-pubs@uow.edu.au

Quasi-orthogonal space-time-frequency codes in MB-OFDM UWB

Abstract

Quasi-Orthogonal Space-Time-Frequency Codes (QOSTFCs) will be examined in this paper to advance either data rate or error performance in recently proposed Space-Time-Frequency Coded Multiband OFDM Ultra-Wideband (STFC MB-OFDM UWB) communication systems. It is shown that QOSTFCs can provide signi¯cantly better error performance, compared to the conventional MB-OFDM UWB (without STFCs) and to the Orthogonal STFCs (OSTFCs) of the same order, at the same data rate, without increasing the total transmission power. Another form of the enhancement would be that QOSTFCs can provide higher data rates with the same error performance, compared to OSTFCs.

Keywords

frequency, quasi, mb, time, ofdm, space, codes, orthogonal, uwb

Disciplines

Physical Sciences and Mathematics

Publication Details

L. Tran, A. Mertins & T. A. Wysocki, "Quasi-orthogonal space-time-frequency codes in MB-OFDM UWB," Computers & Electrical Engineering, vol. 36, (4) pp. 766-774, 2010.

This journal article is available at Research Online: http://ro.uow.edu.au/infopapers/838

Quasi-Orthogonal Space-Time-Frequency Codes in MB-OFDM UWB ⋆

Le Chung Tran [a,*], Alfred Mertins [a], Tadeusz A. Wysocki [b]

[a] *University of Luebeck, Germany*

[b] *University of Nebraska - Lincoln, USA*

Abstract

Quasi-Orthogonal Space-Time-Frequency Codes (QOSTFCs) will be examined in this paper to advance either data rate or error performance in recently proposed Space-Time-Frequency Coded Multiband OFDM Ultra-Wideband (STFC MB-OFDM UWB) communication systems. It is shown that QOSTFCs can provide significantly better error performance, compared to the conventional MB-OFDM UWB (without STFCs) and to the Orthogonal STFCs (OSTFCs) of the same order, at the same data rate, without increasing the total transmission power. Another form of the enhancement would be that QOSTFCs can provide higher data rates with the same error performance, compared to OSTFCs.

Key words:
UWB, MB-OFDM, QOSTFC, STFC, MIMO.

1. Introduction

Combination of the emerging technologies Multiband OFDM Ultra-Wideband (MB-OFDM UWB) [1], Multiple Input Multiple Output (MIMO) [2], and Space-Time Codes (STCs) [3], [4] may improve significantly the maximum achievable wireless communication range, bit error performance, system capacity, data rate or a combined form of those. This combination has been somewhat mentioned in the literature. In particular, the combination of MB-OFDM UWB and Space-Time Block Codes (STBCs) has been mentioned in [5] for only 2 transmit antennas, i.e. the Alamouti code [3]. In [6], the authors proposed a general framework to analyze the performance of MB-OFDM MIMO UWB systems regardless of specific coding schemes in case of Nakagami frequency-selective fading channels. In [7], [8], we proposed the Space-Time-Frequency Coded MB-OFDM UWB (STFC MB-OFDM UWB) system for any number of transmit/reveive (Tx/Rx) antennas (see Fig. 1). We modified Tarokh's proof [4] to quantify the diversity and coding gains of the proposed STFC MB-OFDM UWB system in the log-normal distribution case [9], and then derived the design criteria and maximum likelihood (ML) decoding expressions for STFCs in MB-OFDM UWB. Due to the limited space, an overview of the proposed STFC MB-OFDM UWB system will not be repeated here. We would like to refer readers to [8, Section II], [10, Section II] or [7, Section III] for more detail.

One disadvantage of STFCs that are constructed based directly on complex Orthogonal STBCs (OSTBCs), as mentioned in [7], is the reduced code rate when the number of Tx antennas increases. It is well known that OSTBCs for more than 2 Tx antennas cannot provide the full rate. To increase the code rate of OSTBCs, in [11], the author proposed Quasi-Orthogonal STBCs (QOSTBCs) for 4 and 8 Tx antennas providing higher data rates than the conventional OSTBCs of the same orders, while they still can provide a large (but not full) diversity. Equivalently, QOSTBCs can provide better error performance, compared to OSTBCs of the same order, at the same data rate [11]. The idea of QOSTBCs [11] can definitely be further extended to apply to STFCs in MB-OFDM UWB. Therefore, in this paper, we consider the application of Quasi-Orthogonal STFCs (QOSTFCs), which have higher code rates than orthogonal STFCs (OSTFCs) of the same order, in the proposed STFC MB-OFDM UWB system.

⋆ The material of this work has been partially presented at the IEEE Int. Conf. Sign. Process. & Commun. Syst. (ICSPCS2007), Gold Coast, Australia, Dec. 2007 and at the IEEE Int. Conf. Ultra-Wideband (ICUWB 2008), Hannover, Germany, Sept. 2008.

* Corresponding author.

Email addresses: tran@isip.uni-luebeck.de (Le Chung Tran), mertins@isip.uni-luebeck.de (Alfred Mertins), twysocki@mail.unomaha.edu (Tadeusz A. Wysocki).

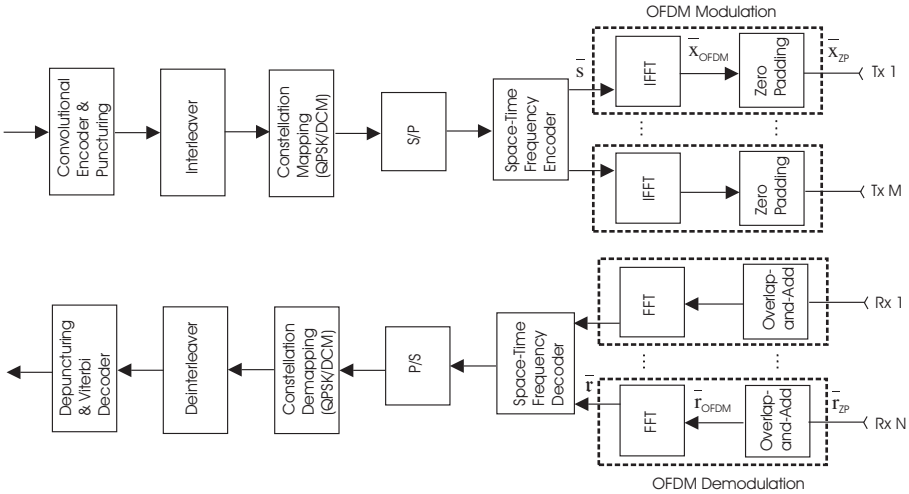

Fig. 1. Structural diagram of the proposed STFC MB-OFDM UWB [7].

It will be shown that, although only partial diversity can be achieved, QOSTFCs may still provide better error performance over OSTFCs of the same order, without any increase of the total transmission power.

The paper is organized as follows. Section 2 analyzes the feasibility of the deployment of QOSTFCs with the order up to 8 in the STFC MB-OFDM system, and derives the examples of QOSTFCs of orders 4 and 8 together with the counterpart OSTFCs for illustration. Section 3 derives the decoding metrics for these OSTFCs and QOSTFCs. In Section 4, simulation results are shown to verify our analysis. Conclusions are drawn in Section 5.

The following notations will be used throughout the paper. The superscript $(.)^*$ denotes the complex conjugation. We denote $\bar{\mathbf{a}} \bullet \bar{\mathbf{b}}$ to be the element-wise (or Hadamard) product of the two vectors $\bar{\mathbf{a}}$ and $\bar{\mathbf{b}}$. N_D and N_{fft} are the number of data sub-carriers and the FFT/IFFT size, respectively (for MB-OFDM UWB communications [1], $N_D = 100$ and $N_{fft} = 128$). Further, $\bar{\mathbf{a}}.\hat{}2$ denotes the element-wise power-2 operation of $\bar{\mathbf{a}}$. The complex space $\mathcal{C}$ of a symbol s denotes all potential possibilities that the symbol s can take, while the N_D-dimensional complex space $\mathcal{C}^{N_D}$ of a length-N_D vector $\bar{\mathbf{s}}$ denotes all potential possibilities that the vector $\bar{\mathbf{s}}$ can take. We define $\bar{\mathbf{1}}$ as a column vector of length N_D, whose elements are all 1. Finally, $\| \, . \, \|_F$ denotes the Frobenius norm.

2. Quasi-Orthogonal STFCs

For the code rate of a STFC [7] being defined as the ratio of the number of transmitted MB-OFDM symbols and the number of time slots required to transmit the whole block of the code, it is known that the Alamouti code [3] can provide a full rate for two Tx antennas, while higher-order codes for more than two Tx antennas cannot provide the full rate. However, they may still provide a higher diversity order than the Alamouti STFC. As a result, the higher-order codes may provide better error performance. Higher order codes also provide potentially higher capacity for the wireless system. We note that, while high-order codes (order 8 or greater) do not bring about a significant increase of the system capacity in the case $N = 1$ Rx antenna (see Fig. 2.2. in [12]), they may significantly increase the system capacity for $N \geq 2$ Rx antennas (see Fig. 2.4. in [12] for instance). Therefore, the implementation of higher-order STFCs for multiple Tx/Rx antennas in STFC MB-OFDM UWB communications is still of our interest.

A question that could be raised is: what is the possible maximum order of STFCs which may be practically applied to MB-OFDM UWB systems? It is well known that Tx antennas should be separated from one another by at least $\lambda/2$, where λ is the UWB wavelength, in order to avoid the spatial correlation between the Tx antennas. For the UWB frequency range 3.1-10.6 GHz, this minimum distance is in the range of 14.2-48.4 mm. Let us consider the implementation of order-8 STFCs (8 Tx antennas are required). The length of UWB devices locating 8 Tx antennas should be about $7\lambda/2$, i.e. in the range 9.9-33.9 cm. This length is the typical length of wireless devices, such as wireless access points or routers. For more than 8 Tx antennas, the physical size of UWB devices might be too large and thus impractical. Therefore, the application of up to 8 Tx antennas can be feasible in STFC MB-OFDM UWB.

As mentioned previously in the introduction, QOSTFCs can be used to improve either the data rate or the error performance of MB-OFDM UWB systems. In particular, for 4 Tx antennas, the following full rate QOSTFC S_{4b}, which is constructed in the similar way as the QOSTBC proposed in [11], can be applied

$$\mathbf{S_{4b}} = \begin{bmatrix} \bar{\mathbf{s}}_1 & \bar{\mathbf{s}}_2 & \bar{\mathbf{s}}_3 & \bar{\mathbf{s}}_4 \\ -\bar{\mathbf{s}}_2^* & \bar{\mathbf{s}}_1^* & -\bar{\mathbf{s}}_4^* & \bar{\mathbf{s}}_3^* \\ -\bar{\mathbf{s}}_3^* & -\bar{\mathbf{s}}_4^* & \bar{\mathbf{s}}_1^* & \bar{\mathbf{s}}_2^* \\ \bar{\mathbf{s}}_4 & -\bar{\mathbf{s}}_3 & -\bar{\mathbf{s}}_2 & \bar{\mathbf{s}}_1 \end{bmatrix}, \tag{1}$$

where $\bar{\mathbf{s}}_i$ denotes a length-N_{fft} column vector, while N_{fft}

is the FFT/IFFT size. This QOSTFC provides a higher code rate with the penalty of loosing half diversity order, compared to the following rate-3/4 OSTFC S_{4a}, which is constructed based on the code proposed in [13] for conventional wireless STBC MIMO systems:

$$\mathbf{S_{4a}} = \begin{bmatrix} \bar{\mathbf{s}}_1 & \bar{\mathbf{s}}_2 & \bar{\mathbf{s}}_3 & 0 \\ -\bar{\mathbf{s}}_2^* & \bar{\mathbf{s}}_1^* & 0 & \bar{\mathbf{s}}_3 \\ -\bar{\mathbf{s}}_3^* & 0 & \bar{\mathbf{s}}_1^* & -\bar{\mathbf{s}}_2 \\ 0 & -\bar{\mathbf{s}}_3^* & \bar{\mathbf{s}}_2^* & \bar{\mathbf{s}}_1 \end{bmatrix}. \quad (2)$$

For 8 Tx antennas, the following rate-3/4 QOSTFC S_{8b} (constructed in the similar way as the QOSTBC proposed in [11]) can be used

$$\mathbf{S_{8b}} = \begin{bmatrix} \bar{\mathbf{s}}_1 & \bar{\mathbf{s}}_2 & \bar{\mathbf{s}}_3 & 0 & \bar{\mathbf{s}}_4 & \bar{\mathbf{s}}_5 & \bar{\mathbf{s}}_6 & 0 \\ -\bar{\mathbf{s}}_2^* & \bar{\mathbf{s}}_1^* & 0 & -\bar{\mathbf{s}}_3 & \bar{\mathbf{s}}_5^* & -\bar{\mathbf{s}}_4^* & 0 & \bar{\mathbf{s}}_6 \\ \bar{\mathbf{s}}_3^* & 0 & -\bar{\mathbf{s}}_1^* & -\bar{\mathbf{s}}_2 & -\bar{\mathbf{s}}_6^* & 0 & \bar{\mathbf{s}}_4^* & \bar{\mathbf{s}}_5 \\ 0 & -\bar{\mathbf{s}}_3^* & \bar{\mathbf{s}}_2^* & -\bar{\mathbf{s}}_1 & 0 & \bar{\mathbf{s}}_6^* & -\bar{\mathbf{s}}_5^* & \bar{\mathbf{s}}_4 \\ -\bar{\mathbf{s}}_4 & -\bar{\mathbf{s}}_5 & -\bar{\mathbf{s}}_6 & 0 & \bar{\mathbf{s}}_1 & \bar{\mathbf{s}}_2 & \bar{\mathbf{s}}_3 & 0 \\ -\bar{\mathbf{s}}_5^* & \bar{\mathbf{s}}_4^* & 0 & \bar{\mathbf{s}}_6 & -\bar{\mathbf{s}}_2^* & \bar{\mathbf{s}}_1^* & 0 & \bar{\mathbf{s}}_3 \\ \bar{\mathbf{s}}_6^* & 0 & -\bar{\mathbf{s}}_4^* & \bar{\mathbf{s}}_5 & \bar{\mathbf{s}}_3^* & 0 & -\bar{\mathbf{s}}_1^* & \bar{\mathbf{s}}_2 \\ 0 & \bar{\mathbf{s}}_6^* & -\bar{\mathbf{s}}_5^* & -\bar{\mathbf{s}}_4 & 0 & \bar{\mathbf{s}}_3^* & -\bar{\mathbf{s}}_2^* & -\bar{\mathbf{s}}_1 \end{bmatrix}. \quad (3)$$

This QOSTFC provides a higher code rate with the penalty of loosing a portion of maximum diversity order, compared to the following rate-1/2 OSTFC S_{8a}, which is constructed based on the code proposed in [13] for conventional wireless STBC MIMO systems:

$$\mathbf{S_{8a}} = \begin{bmatrix} \bar{\mathbf{s}}_1 & -\bar{\mathbf{s}}_2^* & -\bar{\mathbf{s}}_3^* & 0 & -\bar{\mathbf{s}}_4^* & 0 & 0 & 0 \\ \bar{\mathbf{s}}_2 & \bar{\mathbf{s}}_1^* & 0 & \bar{\mathbf{s}}_3^* & 0 & \bar{\mathbf{s}}_4^* & 0 & 0 \\ \bar{\mathbf{s}}_3 & 0 & \bar{\mathbf{s}}_1^* & -\bar{\mathbf{s}}_2^* & 0 & 0 & \bar{\mathbf{s}}_4^* & 0 \\ 0 & -\bar{\mathbf{s}}_3 & \bar{\mathbf{s}}_2 & \bar{\mathbf{s}}_1 & 0 & 0 & 0 & -\bar{\mathbf{s}}_4^* \\ \bar{\mathbf{s}}_4 & 0 & 0 & 0 & \bar{\mathbf{s}}_1^* & -\bar{\mathbf{s}}_2^* & -\bar{\mathbf{s}}_3^* & 0 \\ 0 & -\bar{\mathbf{s}}_4 & 0 & 0 & \bar{\mathbf{s}}_2 & \bar{\mathbf{s}}_1 & 0 & \bar{\mathbf{s}}_3^* \\ 0 & 0 & -\bar{\mathbf{s}}_4 & 0 & \bar{\mathbf{s}}_3 & 0 & \bar{\mathbf{s}}_1 & -\bar{\mathbf{s}}_2^* \\ 0 & 0 & 0 & \bar{\mathbf{s}}_4 & 0 & -\bar{\mathbf{s}}_3 & \bar{\mathbf{s}}_2 & \bar{\mathbf{s}}_1^* \end{bmatrix}. \quad (4)$$

It can be realized that the columns ν_i, for $i = 1, \ldots 8$, of S_{8b} are orthogonal, except for the pairs (ν_1, ν_5), (ν_2, ν_6) and (ν_3, ν_7). Clearly, the orthogonality of S_{8b} (thus the diversity) is partially released to achieve the higher rate.

3. Decoding Metrics

We now derive the ML decoding metrics for the above OSTFCs and QOSTFCs in a MIMO system with N Rx antennas, using a PSK or QAM modulation scheme. Let us consider the two codes $\mathbf{S}_{4a}$ and $\mathbf{S}_{4b}$ as examples. Because $\mathbf{S}$ is completely orthogonal (for $\mathbf{S}_{4a}$) or partially orthogonal (for $\mathbf{S}_{4b}$), each MB-OFDM symbol can be decoded separately for the code $\mathbf{S}_{4a}$, while a pair of MB-OFDM symbols must be decoded at a time for the code $\mathbf{S}_{4b}$. The decoding metrics of MB-OFDM symbols in the two codes can be easily found based on the decoding metrics of the respective OSTBC (see, for example, [12, Section 3.3]) and QOSTBC [11, Section III]. Furthermore, instead of having to decode jointly the whole N_D data points corresponding to the N_D data sub-carriers ($N_D = 100$ according to [1]) within a MB-OFDM symbol $\bar{\mathbf{s}}_{t,m}$, each data point among these N_D data sub-carriers (a pair of data points for QOSTFCs) can be decoded separately. Thus the decoding process is relatively simple. The decoding metrics of MB-OFDM symbols for $\mathbf{S}_{4a}$, $\mathbf{S}_{4b}$, $\mathbf{S}_{8a}$ and $\mathbf{S}_{8b}$ are presented in Tables 1, 2, 3 and 4, respectively. In these tables, $\bar{\mathfrak{h}}_{m,n}$ is the column vector obtained by applying the FFT to the respective channel coefficient vector $\bar{\mathbf{h}}_{m,n}$, i.e. $\bar{\mathfrak{h}}_{m,n} = FFT\{\bar{\mathbf{h}}_{m,n}\}$, while $\bar{\mathfrak{r}}_{m,n}$ is the column vector of received signals at the output of the FFT blocks in Fig. 1. Once again, we refer readers to [7, Section III A] for more detail about how these vectors are formed.

From Tables 1 and 3 (Tables 2 and 4, respectively), the data at each tone (a pair of data at each tone) can be decoded separately, rather than jointly. For illustration, let us consider the simple case where we have $N = 1$ Rx an-

Table 1
Decoding Metrics for $\mathbf{S_{4a}}$ with PSK or QAM Modulations.

Symbol	Decoding Metric
$\bar{\mathbf{s}}_1$	$\arg\min_{\bar{\mathbf{s}}\in\mathcal{C}^{N_D}} \parallel \Big[\Big\| \sum_{n=1}^{N} \big(\bar{\mathfrak{h}}_{2,n} \bullet \bar{\mathfrak{r}}_{2,n}^* + \bar{\mathfrak{h}}_{3,n} \bullet \bar{\mathfrak{r}}_{3,n}^* + \bar{\mathfrak{h}}_{1,n}^* \bullet \bar{\mathfrak{r}}_{1,n} + \bar{\mathfrak{h}}_{4,n}^* \bullet \bar{\mathfrak{r}}_{4,n}\big) - \bar{\mathbf{s}}\Big\|.\hat{}\,2 + (-\bar{\mathbf{1}} + \sum_{m=1}^{4}\sum_{n=1}^{N} \|\bar{\mathfrak{h}}_{m,n}\|.\hat{}\,2) \bullet (\|\bar{\mathbf{s}}\|.\hat{}\,2)\Big] \parallel_F^2$
$\bar{\mathbf{s}}_2$	$\arg\min_{\bar{\mathbf{s}}\in\mathcal{C}^{N_D}} \parallel \Big[\Big\| \sum_{n=1}^{N} \big(-\bar{\mathfrak{h}}_{2,n}^* \bullet \bar{\mathfrak{r}}_{1,n} - \bar{\mathfrak{h}}_{4,n}^* \bullet \bar{\mathfrak{r}}_{3,n} - \bar{\mathfrak{h}}_{1,n} \bullet \bar{\mathfrak{r}}_{2,n}^* + \bar{\mathfrak{h}}_{3,n} \bullet \bar{\mathfrak{r}}_{4,n}^*\big) - \bar{\mathbf{s}}\Big\|.\hat{}\,2 + (-\bar{\mathbf{1}} + \sum_{m=1}^{4}\sum_{n=1}^{N} \|\bar{\mathfrak{h}}_{m,n}\|.\hat{}\,2) \bullet (\|\bar{\mathbf{s}}\|.\hat{}\,2)\Big] \parallel_F^2$
$\bar{\mathbf{s}}_3$	$\arg\min_{\bar{\mathbf{s}}\in\mathcal{C}^{N_D}} \parallel \Big[\Big\| \sum_{n=1}^{N} \big(-\bar{\mathfrak{h}}_{1,n} \bullet \bar{\mathfrak{r}}_{3,n}^* - \bar{\mathfrak{h}}_{2,n} \bullet \bar{\mathfrak{r}}_{4,n}^* + \bar{\mathfrak{h}}_{3,n}^* \bullet \bar{\mathfrak{r}}_{1,n} + \bar{\mathfrak{h}}_{4,n}^* \bullet \bar{\mathfrak{r}}_{2,n}\big) - \bar{\mathbf{s}}\Big\|.\hat{}\,2 + (-\bar{\mathbf{1}} + \sum_{m=1}^{4}\sum_{n=1}^{N} \|\bar{\mathfrak{h}}_{m,n}\|.\hat{}\,2) \bullet (\|\bar{\mathbf{s}}\|.\hat{}\,2)\Big] \parallel_F^2$

Table 2
Decoding Metrics for $\mathbf{S_{4b}}$ with PSK or QAM Modulations.

Symbols	Decoding Metric
$(\bar{\mathbf{s}}_1, \bar{\mathbf{s}}_4)$	$\arg\min_{\bar{\mathbf{s}}_1,\bar{\mathbf{s}}_4\in\mathcal{C}^{N_D}} \parallel \Big(\sum_{m=1}^{4}\sum_{n=1}^{N} \|\bar{\mathfrak{h}}_{m,n}\|.\hat{}\,2\Big) \bullet (\|\bar{\mathbf{s}}_1\|.\hat{}\,2 + \|\bar{\mathbf{s}}_4\|.\hat{}\,2) + 2Real[\sum_{n=1}^{N}(-\bar{\mathfrak{h}}_{1,n} \bullet \bar{\mathfrak{r}}_{1,n}^* - \bar{\mathfrak{h}}_{2,n}^* \bullet \bar{\mathfrak{r}}_{2,n} - \bar{\mathfrak{h}}_{3,n}^* \bullet \bar{\mathfrak{r}}_{3,n} - \bar{\mathfrak{h}}_{4,n} \bullet \bar{\mathfrak{r}}_{4,n}^*) \bullet \bar{\mathbf{s}}_1] + 2Real[\sum_{n=1}^{N}(-\bar{\mathfrak{h}}_{4,n} \bullet \bar{\mathfrak{r}}_{1,n}^* + \bar{\mathfrak{h}}_{3,n}^* \bullet \bar{\mathfrak{r}}_{2,n} + \bar{\mathfrak{h}}_{2,n}^* \bullet \bar{\mathfrak{r}}_{3,n} - \bar{\mathfrak{h}}_{1,n} \bullet \bar{\mathfrak{r}}_{4,n}^*) \bullet \bar{\mathbf{s}}_4] + 2Real[\sum_{n=1}^{N}(\bar{\mathfrak{h}}_{1,n} \bullet \bar{\mathfrak{h}}_{4,n}^* - \bar{\mathfrak{h}}_{2,n}^* \bullet \bar{\mathfrak{h}}_{3,n} - \bar{\mathfrak{h}}_{2,n} \bullet \bar{\mathfrak{h}}_{3,n}^* + \bar{\mathfrak{h}}_{1,n}^* \bullet \bar{\mathfrak{h}}_{4,n}) \bullet \bar{\mathbf{s}}_1 \bullet \bar{\mathbf{s}}_4^*] \parallel_F^2$
$(\bar{\mathbf{s}}_2, \bar{\mathbf{s}}_3)$	$\arg\min_{\bar{\mathbf{s}}_2,\bar{\mathbf{s}}_3\in\mathcal{C}^{N_D}} \parallel \Big(\sum_{m=1}^{4}\sum_{n=1}^{N} \|\bar{\mathfrak{h}}_{m,n}\|.\hat{}\,2\Big) \bullet (\|\bar{\mathbf{s}}_2\|.\hat{}\,2 + \|\bar{\mathbf{s}}_3\|.\hat{}\,2) + 2Real[\sum_{n=1}^{N}(-\bar{\mathfrak{h}}_{2,n} \bullet \bar{\mathfrak{r}}_{1,n}^* + \bar{\mathfrak{h}}_{1,n}^* \bullet \bar{\mathfrak{r}}_{2,n} - \bar{\mathfrak{h}}_{4,n}^* \bullet \bar{\mathfrak{r}}_{3,n} + \bar{\mathfrak{h}}_{3,n} \bullet \bar{\mathfrak{r}}_{4,n}^*) \bullet \bar{\mathbf{s}}_2] + 2Real[\sum_{n=1}^{N}(-\bar{\mathfrak{h}}_{3,n} \bullet \bar{\mathfrak{r}}_{1,n}^* - \bar{\mathfrak{h}}_{4,n}^* \bullet \bar{\mathfrak{r}}_{2,n} + \bar{\mathfrak{h}}_{1,n}^* \bullet \bar{\mathfrak{r}}_{3,n} + \bar{\mathfrak{h}}_{2,n} \bullet \bar{\mathfrak{r}}_{4,n}^*) \bullet \bar{\mathbf{s}}_3] + 2Real[\sum_{n=1}^{N}(\bar{\mathfrak{h}}_{2,n} \bullet \bar{\mathfrak{h}}_{3,n}^* - \bar{\mathfrak{h}}_{1,n}^* \bullet \bar{\mathfrak{h}}_{4,n} - \bar{\mathfrak{h}}_{1,n} \bullet \bar{\mathfrak{h}}_{4,n}^* + \bar{\mathfrak{h}}_{2,n}^* \bullet \bar{\mathfrak{h}}_{3,n}) \bullet \bar{\mathbf{s}}_2 \bullet \bar{\mathbf{s}}_3^*] \parallel_F^2$

Table 3
Decoding Metrics for $\mathbf{S_{8a}}$ with PSK or QAM Modulations.

Symbol	Decoding Metric
$\bar{\mathbf{s}}_1$	$\arg\min_{\bar{\mathbf{s}}\in\mathcal{C}^{N_D}} \Big\Vert \Big[\Big\vert \sum_{n=1}^{N}\Big(\bar{\mathfrak{h}}_{5,n}\bullet\bar{\mathfrak{r}}^*_{5,n}+\bar{\mathfrak{h}}_{2,n}\bullet\bar{\mathfrak{r}}^*_{2,n}+ \bar{\mathfrak{h}}^*_{1,n}\bullet\bar{\mathfrak{r}}_{1,n}+\bar{\mathfrak{h}}^*_{4,n}\bullet\bar{\mathfrak{r}}_{4,n}+\bar{\mathfrak{h}}_{3,n}\bullet\bar{\mathfrak{r}}^*_{3,n}+\bar{\mathfrak{h}}_{8,n}\bullet\bar{\mathfrak{r}}^*_{8,n}+ \bar{\mathfrak{h}}^*_{6,n}\bullet\bar{\mathfrak{r}}_{6,n}+\bar{\mathfrak{h}}^*_{7,n}\bullet\bar{\mathfrak{r}}_{7,n}\Big)-\bar{\mathbf{s}}\Big\vert.\hat{}\,2+ (-\bar{\mathbf{1}}+\sum_{m=1}^{8}\sum_{n=1}^{N}\vert\bar{\mathfrak{h}}_{m,n}\vert.\hat{}\,2)\bullet(\vert\bar{\mathbf{s}}\vert.\hat{}\,2)\Big]\Big\Vert_F^2$
$\bar{\mathbf{s}}_2$	$\arg\min_{\bar{\mathbf{s}}\in\mathcal{C}^{N_D}} \Big\Vert \Big[\Big\vert \sum_{n=1}^{N}\Big(-\bar{\mathfrak{h}}_{8,n}\bullet\bar{\mathfrak{r}}^*_{7,n}-\bar{\mathfrak{h}}_{2,n}\bullet\bar{\mathfrak{r}}^*_{1,n}- \bar{\mathfrak{h}}_{6,n}\bullet\bar{\mathfrak{r}}^*_{5,n}+\bar{\mathfrak{h}}^*_{5,n}\bullet\bar{\mathfrak{r}}_{6,n}+\bar{\mathfrak{h}}^*_{7,n}\bullet\bar{\mathfrak{r}}_{8,n}+\bar{\mathfrak{h}}^*_{1,n}\bullet\bar{\mathfrak{r}}_{2,n}+ \bar{\mathfrak{h}}^*_{3}\bullet\bar{\mathfrak{r}}_{4}-\bar{\mathfrak{h}}_{4}\bullet\bar{\mathfrak{r}}^*_{3}\Big)-\bar{\mathbf{s}}\Big\vert.\hat{}\,2+ (-\bar{\mathbf{1}}+\sum_{m=1}^{8}\sum_{n=1}^{N}\vert\bar{\mathfrak{h}}_{m,n}\vert.\hat{}\,2)\bullet(\vert\bar{\mathbf{s}}\vert.\hat{}\,2)\Big]\Big\Vert_F^2$
$\bar{\mathbf{s}}_3$	$\arg\min_{\bar{\mathbf{s}}\in\mathcal{C}^{N_D}} \Big\Vert \Big[\Big\vert \sum_{n=1}^{N}\Big(\bar{\mathfrak{h}}_{8,n}\bullet\bar{\mathfrak{r}}^*_{6,n}-\bar{\mathfrak{h}}_{3,n}\bullet\bar{\mathfrak{r}}^*_{1,n}+ \bar{\mathfrak{h}}^*_{1,n}\bullet\bar{\mathfrak{r}}_{3,n}-\bar{\mathfrak{h}}^*_{2,n}\bullet\bar{\mathfrak{r}}_{4,n}+\bar{\mathfrak{h}}_{4,n}\bullet\bar{\mathfrak{r}}^*_{2,n}-\bar{\mathfrak{h}}_{7,n}\bullet\bar{\mathfrak{r}}^*_{5,n}+ \bar{\mathfrak{h}}^*_{5,n}\bullet\bar{\mathfrak{r}}_{7,n}-\bar{\mathfrak{h}}^*_{6,n}\bullet\bar{\mathfrak{r}}_{8,n}\Big)-\bar{\mathbf{s}}\Big\vert.\hat{}\,2+ (-\bar{\mathbf{1}}+\sum_{m=1}^{8}\sum_{n=1}^{N}\vert\bar{\mathfrak{h}}_{m,n}\vert.\hat{}\,2)\bullet(\vert\bar{\mathbf{s}}\vert.\hat{}\,2)\Big]\Big\Vert_F^2$
$\bar{\mathbf{s}}_4$	$\arg\min_{\bar{\mathbf{s}}\in\mathcal{C}^{N_D}} \Big\Vert \Big[\Big\vert \sum_{n=1}^{N}\Big(-\bar{\mathfrak{h}}_{8,n}\bullet\bar{\mathfrak{r}}^*_{4,n}+\bar{\mathfrak{h}}_{7,n}\bullet\bar{\mathfrak{r}}^*_{3,n}- \bar{\mathfrak{h}}_{5,n}\bullet\bar{\mathfrak{r}}^*_{1,n}+\bar{\mathfrak{h}}_{6,n}\bullet\bar{\mathfrak{r}}^*_{2,n}+\bar{\mathfrak{h}}^*_{1,n}\bullet\bar{\mathfrak{r}}_{5,n}-\bar{\mathfrak{h}}^*_{2,n}\bullet\bar{\mathfrak{r}}_{6,n}- \bar{\mathfrak{h}}^*_{3,n}\bullet\bar{\mathfrak{r}}_{7,n}+\bar{\mathfrak{h}}^*_{4,n}\bullet\bar{\mathfrak{r}}_{8,n}\Big)-\bar{\mathbf{s}}\Big\vert.\hat{}\,2+ (-\bar{\mathbf{1}}+\sum_{m=1}^{8}\sum_{n=1}^{N}\vert\bar{\mathfrak{h}}_{m,n}\vert.\hat{}\,2)\bullet(\vert\bar{\mathbf{s}}\vert.\hat{}\,2)\Big]\Big\Vert_F^2$

tenna, thus the subscript n can be omitted for brevity. Denote $\hbar_{m,k}$ and $\mathfrak{r}_{m,k}$ to be the k-th element of the column vectors $\bar{\mathfrak{h}}_m$ and $\bar{\mathfrak{r}}_m$, respectively. From Table 1, the decoding metric for data at the k-th data sub-carrier (or tone), for $k = 1, \ldots, N_D$, in the MB-OFDM symbol $\bar{\mathbf{s}}_1$ of $\mathbf{S}_{4a}$ is

$$s_{1,k} = \arg\min_{s\in\mathcal{C}} \Big[\Big\vert\big(\hbar_{2,k}\mathfrak{r}^*_{2,k}+\hbar_{3,k}\mathfrak{r}^*_{3,k}+\hbar^*_{1,k}\mathfrak{r}_{1,k}+ \hbar^*_{4,k}\mathfrak{r}_{4,k}\big)-s\Big\vert^2+(-1+\sum_{m=1}^{4}\vert\hbar_{m,k}\vert^2)\vert s\vert^2\Big] \tag{5}$$

while, from Table 2, the decoding metric for a pair of data at the k-th data sub-carrier, within the MB-OFDM symbols $\bar{\mathbf{s}}_1$ and $\bar{\mathbf{s}}_4$ of $\mathbf{S}_{4b}$ is

$$\begin{aligned}(s_{1,k}, s_{4,k}) = \arg\min_{s_1,s_4\in\mathcal{C}} \big(\sum_{m=1}^{4}\vert\hbar_{m,k}\vert^2\big)(\vert s_1\vert^2+\vert s_4\vert^2)+ \\ 2Real[(-\hbar_{1,k}\mathfrak{r}^*_{1,k}-\hbar^*_{2,k}\mathfrak{r}_{2,k}-\hbar^*_{3,k}\mathfrak{r}_{3,k}- \\ \hbar_{4,k}\mathfrak{r}^*_{4,k})s_1]+2Real[(-\hbar_{4,k}\mathfrak{r}^*_{1,k}+\hbar^*_{3,k}\mathfrak{r}_{2,k}+ \\ \hbar^*_{2,k}\mathfrak{r}_{3,k}-\hbar_{1,k}\mathfrak{r}^*_{4,k})s_4]+2Real[(\hbar_{1,k}\hbar^*_{4,k}- \\ \hbar^*_{2,k}\hbar_{3,k}-\hbar_{2,k}\hbar^*_{3,k}+\hbar^*_{1,k}\hbar_{4,k})s_1s^*_4]\end{aligned} \tag{6}$$

We recall that the searches in the aforementioned decoding metrics are carried out over all potential possibilities of the symbol(s) s in (5) (s_1, s_4 in (6), respectively) in the original PSK or QAM signal constellations. It is clear from the above examples that the decoding metrics are relatively simple.

Table 4
Decoding Metrics for $\mathbf{S_{8b}}$ with PSK or QAM Modulations.

Symbols	Decoding Metric
$(\bar{\mathbf{s}}_1, \bar{\mathbf{s}}_4)$	$\arg\min_{\bar{\mathbf{s}}_1,\bar{\mathbf{s}}_4\in\mathcal{C}^{N_D}} \Big\Vert \Big(\sum_{m=1}^{8}\sum_{n=1}^{N}\vert\bar{\mathfrak{h}}_{m,n}\vert.\hat{}\,2\Big)\bullet(\vert\bar{\mathbf{s}}_1\vert.\hat{}\,2+ \vert\bar{\mathbf{s}}_4\vert.\hat{}\,2)+2Real[\sum_{n=1}^{N}(-\bar{\mathfrak{h}}^*_{6,n}\bullet\bar{\mathfrak{r}}_{6,n}+\bar{\mathfrak{h}}_{4,n}\bullet\bar{\mathfrak{r}}^*_{4,n}+ \bar{\mathfrak{h}}^*_{3,n}\bullet\bar{\mathfrak{r}}_{3,n}-\bar{\mathfrak{h}}^*_{2,n}\bullet\bar{\mathfrak{r}}_{2,n}+\bar{\mathfrak{h}}_{8,n}\bullet\bar{\mathfrak{r}}^*_{8,n}-\bar{\mathfrak{h}}_{1,n}\bullet\bar{\mathfrak{r}}^*_{1,n}- \bar{\mathfrak{h}}_{5,n}\bullet\bar{\mathfrak{r}}^*_{5,n}+\bar{\mathfrak{h}}^*_{7,n}\bullet\bar{\mathfrak{r}}_{7,n})\bullet\bar{\mathbf{s}}_1]+2Real[\sum_{n=1}^{N}(\bar{\mathfrak{h}}_{4,n}\bullet\bar{\mathfrak{r}}^*_{8,n}+ \bar{\mathfrak{h}}^*_{6,n}\bullet\bar{\mathfrak{r}}_{2,n}+\bar{\mathfrak{h}}_{1,n}\bullet\bar{\mathfrak{r}}^*_{5,n}+\bar{\mathfrak{h}}^*_{3,n}\bullet\bar{\mathfrak{r}}_{7,n}-\bar{\mathfrak{h}}^*_{2,n}\bullet\bar{\mathfrak{r}}_{6,n}- \bar{\mathfrak{h}}^*_{7,n}\bullet\bar{\mathfrak{r}}_{3,n}-\bar{\mathfrak{h}}_{8,n}\bullet\bar{\mathfrak{r}}^*_{4,n}-\bar{\mathfrak{h}}_{5,n}\bullet\bar{\mathfrak{r}}^*_{1,n})\bullet\bar{\mathbf{s}}_4]+ 2Real[\sum_{n=1}^{N}(-\bar{\mathfrak{h}}^*_{1,n}\bullet\bar{\mathfrak{h}}_{5,n}-\bar{\mathfrak{h}}_{4,n}\bullet\bar{\mathfrak{h}}^*_{8,n}+\bar{\mathfrak{h}}^*_{4,n}\bullet\bar{\mathfrak{h}}_{8,n}- \bar{\mathfrak{h}}^*_{2,n}\bullet\bar{\mathfrak{h}}_{6,n}+\bar{\mathfrak{h}}_{1,n}\bullet\bar{\mathfrak{h}}^*_{5,n}-\bar{\mathfrak{h}}^*_{3,n}\bullet\bar{\mathfrak{h}}_{7,n}+\bar{\mathfrak{h}}_{2,n}\bullet\bar{\mathfrak{h}}^*_{6,n}+ \bar{\mathfrak{h}}_{3,n}\bullet\bar{\mathfrak{h}}^*_{7,n})\bullet\bar{\mathbf{s}}_1\bullet\bar{\mathbf{s}}^*_4]\Big\Vert_F^2$
$(\bar{\mathbf{s}}_2, \bar{\mathbf{s}}_5)$	$\arg\min_{\bar{\mathbf{s}}_2,\bar{\mathbf{s}}_5\in\mathcal{C}^{N_D}} \Big\Vert \Big(\sum_{m=1}^{8}\sum_{n=1}^{N}\vert\bar{\mathfrak{h}}_{m,n}\vert.\hat{}\,2\Big)\bullet(\vert\bar{\mathbf{s}}_2\vert.\hat{}\,2+ \vert\bar{\mathbf{s}}_5\vert.\hat{}\,2)+2Real[\sum_{n=1}^{N}(\bar{\mathfrak{h}}^*_{5,n}\bullet\bar{\mathfrak{r}}_{6,n}-\bar{\mathfrak{h}}^*_{3,n}\bullet\bar{\mathfrak{r}}_{4,n}+ \bar{\mathfrak{h}}^*_{7,n}\bullet\bar{\mathfrak{r}}_{8,n}+\bar{\mathfrak{h}}^*_{1,n}\bullet\bar{\mathfrak{r}}_{2,n}-\bar{\mathfrak{h}}_{8,n}\bullet\bar{\mathfrak{r}}^*_{7,n}-\bar{\mathfrak{h}}_{6,n}\bullet\bar{\mathfrak{r}}^*_{5,n}- \bar{\mathfrak{h}}_{2,n}\bullet\bar{\mathfrak{r}}^*_{1,n}+\bar{\mathfrak{h}}_{4,n}\bullet\bar{\mathfrak{r}}^*_{3,n})\bullet\bar{\mathbf{s}}_2]+2Real[\sum_{n=1}^{N}(\bar{\mathfrak{h}}^*_{1,n}\bullet\bar{\mathfrak{r}}_{6,n}+ \bar{\mathfrak{h}}_{2,n}\bullet\bar{\mathfrak{r}}^*_{5,n}-\bar{\mathfrak{h}}^*_{5,n}\bullet\bar{\mathfrak{r}}_{2,n}-\bar{\mathfrak{h}}_{4,n}\bullet\bar{\mathfrak{r}}^*_{7,n}+\bar{\mathfrak{h}}^*_{7,n}\bullet\bar{\mathfrak{r}}_{4,n}+ \bar{\mathfrak{h}}^*_{3,n}\bullet\bar{\mathfrak{r}}_{8,n}-\bar{\mathfrak{h}}_{6,n}\bullet\bar{\mathfrak{r}}^*_{1,n}-\bar{\mathfrak{h}}_{8,n}\bullet\bar{\mathfrak{r}}^*_{3,n})\bullet\bar{\mathbf{s}}_5]+ 2Real[\sum_{n=1}^{N}(-\bar{\mathfrak{h}}^*_{2,n}\bullet\bar{\mathfrak{h}}_{6,n}+\bar{\mathfrak{h}}_{1,n}\bullet\bar{\mathfrak{h}}^*_{5,n}+\bar{\mathfrak{h}}_{3,n}\bullet\bar{\mathfrak{h}}^*_{7,n}- \bar{\mathfrak{h}}^*_{3,n}\bullet\bar{\mathfrak{h}}_{7,n}+\bar{\mathfrak{h}}^*_{4,n}\bullet\bar{\mathfrak{h}}_{8,n}-\bar{\mathfrak{h}}_{4,n}\bullet\bar{\mathfrak{h}}^*_{8,n}+\bar{\mathfrak{h}}_{2,n}\bullet\bar{\mathfrak{h}}^*_{6,n}- \bar{\mathfrak{h}}^*_{1,n}\bullet\bar{\mathfrak{h}}_{5,n})\bullet\bar{\mathbf{s}}_2\bullet\bar{\mathbf{s}}^*_5]\Big\Vert_F^2$
$(\bar{\mathbf{s}}_3, \bar{\mathbf{s}}_6)$	$\arg\min_{\bar{\mathbf{s}}_3,\bar{\mathbf{s}}_6\in\mathcal{C}^{N_D}} \Big\Vert \Big(\sum_{m=1}^{8}\sum_{n=1}^{N}\vert\bar{\mathfrak{h}}_{m,n}\vert.\hat{}\,2\Big)\bullet(\vert\bar{\mathbf{s}}_3\vert.\hat{}\,2+ \vert\bar{\mathbf{s}}_6\vert.\hat{}\,2)+2Real[\sum_{n=1}^{N}(-\bar{\mathfrak{h}}_{3,n}\bullet\bar{\mathfrak{r}}^*_{1,n}-\bar{\mathfrak{h}}_{8,n}\bullet\bar{\mathfrak{r}}^*_{6,n}- \bar{\mathfrak{h}}_{7,n}\bullet\bar{\mathfrak{r}}^*_{5,n}+\bar{\mathfrak{h}}^*_{2,n}\bullet\bar{\mathfrak{r}}_{4,n}-\bar{\mathfrak{h}}^*_{1,n}\bullet\bar{\mathfrak{r}}_{3,n}-\bar{\mathfrak{h}}^*_{6,n}\bullet\bar{\mathfrak{r}}_{8,n}- \bar{\mathfrak{h}}^*_{5,n}\bullet\bar{\mathfrak{r}}_{7,n}+\bar{\mathfrak{h}}_{4,n}\bullet\bar{\mathfrak{r}}^*_{2,n})\bullet\bar{\mathbf{s}}_3]+2Real[\sum_{n=1}^{N}(\bar{\mathfrak{h}}_{3,n}\bullet\bar{\mathfrak{r}}^*_{5,n}- \bar{\mathfrak{h}}^*_{2,n}\bullet\bar{\mathfrak{r}}_{8,n}-\bar{\mathfrak{h}}_{8,n}\bullet\bar{\mathfrak{r}}^*_{2,n}-\bar{\mathfrak{h}}_{7,n}\bullet\bar{\mathfrak{r}}^*_{1,n}+\bar{\mathfrak{h}}^*_{5,n}\bullet\bar{\mathfrak{r}}_{3,n}- \bar{\mathfrak{h}}^*_{1,n}\bullet\bar{\mathfrak{r}}_{7,n}-\bar{\mathfrak{h}}^*_{6,n}\bullet\bar{\mathfrak{r}}_{4,n}-\bar{\mathfrak{h}}_{4,n}\bullet\bar{\mathfrak{r}}^*_{6,n})\bullet\bar{\mathbf{s}}_6]+ 2Real[\sum_{n=1}^{N}(-\bar{\mathfrak{h}}_{4,n}\bullet\bar{\mathfrak{h}}^*_{8,n}-\bar{\mathfrak{h}}^*_{3,n}\bullet\bar{\mathfrak{h}}_{7,n}+\bar{\mathfrak{h}}^*_{4,n}\bullet\bar{\mathfrak{h}}_{8,n}+ \bar{\mathfrak{h}}_{3,n}\bullet\bar{\mathfrak{h}}^*_{7,n}-\bar{\mathfrak{h}}^*_{1,n}\bullet\bar{\mathfrak{h}}_{5,n}-\bar{\mathfrak{h}}^*_{2,n}\bullet\bar{\mathfrak{h}}_{6,n}+\bar{\mathfrak{h}}_{1,n}\bullet\bar{\mathfrak{h}}^*_{5}+ \bar{\mathfrak{h}}_{2,n}\bullet\bar{\mathfrak{h}}^*_{6,n})\bullet\bar{\mathbf{s}}_3\bullet\bar{\mathbf{s}}^*_6]\Big\Vert_F^2$

4. Simulation Results

Several Monte-Carlo simulations were run in Matlab^{TM} for the conventional baseband MB-OFDM system without STFCs and for the baseband MB-OFDM with $\mathbf{S}_{4a}$, $\mathbf{S}_{4b}$, $\mathbf{S}_{8a}$, and $\mathbf{S}_{8b}$, at the bit rate 480 Mbps for illustration. Each run of simulations was carried out with 1800 MB-OFDM symbols. One hundred channel realizations of each channel model (CM 1 to CM 4) were considered for the transmission of each MB-OFDM symbol. The channel realizations were created by the Matlab program enclosed in the appendix of the IEEE 802.15.3a channel modeling sub-committee report [9]. The simulation parameters are listed in Table 5. In simulations, SNR is defined to be the signal-to-noise ratio (dB) per sample in a MB-OFDM symbol (consisting of 165 samples), at each Rx antenna, i.e. SNR is the subtraction between the total power (dB) of the received signal corresponding to the sample of interest and the power of noise (dB) at that Rx antenna. To fairly compare the error performance of MB-OFDM systems with and without STFCs, the following two constraints were imposed:

Power constraint: the average power of the signal constellation points is multiplied with a factor of 1 for the un-

Table 5
Simulation Parameters.

Parameter	Value
FFT and IFFT size	$N_{fft} = 128$
Data rate	480 Mbps
Conv. encoder's rate	1/2
Conv. encoder's constraint length	$K = 7$
Conv. decoder	Viterbi
Decoding mode	Hard
No. transmitted MB-OFDM symbols	1800
Modulation	8PSK, 16QAM and 64QAM
IEEE Channel model	CM1, 2, 3 & 4
No. data subcarriers	$N_D = 100$
No. pilot subcarriers	$N_P = 12$
No. guard subcarriers	$N_G = 10$
Total number of subcarriers used	$N_T = 122$
Number of samples in ZPS	$N_{ZPS} = 37$
Total number of samples/symbol	$N_{SYM} = 165$
Number of channel realizations	100

coded MB-OFDM, 1/3 for $\mathbf{S}_{4a}$, 1/4 for $\mathbf{S}_{4b}$, 1/4 for $\mathbf{S}_{8a}$, and 1/6 for $\mathbf{S}_{8b}$. Thereby, the *total transmission power* from all Tx antennas at a certain time is the same for all cases.

Data rate constraint: a suitable modulation scheme is selected for each MB-OFDM system in order to achieve the *same data rate*. To illustrate an example of how to achieve the same date rate for different MB-OFDM systems, we consider a conventional baseband uncoded MB-OFDM system of data rate 320 Mbps with the convolutional encoder's rate of 1/2 and the modulation scheme of either QPSK or DCM (Dual Carrier Modulation [1]). This system is considered as a reference. To have the uncoded MB-OFDM system of data rate 480 Mbps, we maintain all functional blocks, including the convolutional encoder, in this reference system, except for the modulation and demodulation blocks. Particularly, an 8PSK modulation scheme is selected, instead of QPSK or DCM. In a similar manner, a 16QAM modulation scheme is selected when the reference MB-OFDM system is associated with the rate-3/4 STFC $\mathbf{S}_{4a}$ to have the date rate of 480 Mbps. Similarly, we can select 8PSK, 64QAM and 16QAM modulation schemes for the reference MB-OFDM system associated with $\mathbf{S}_{4b}$, $\mathbf{S}_{8a}$ and $\mathbf{S}_{8b}$, respectively, to have the same data rate of 480 Mbps because $\mathbf{S}_{4b}$, $\mathbf{S}_{8a}$ and $\mathbf{S}_{8b}$ have the code rates of 1, 1/2 and 3/4 respectively.

Figs. 2 and 3 compare the error performances in a MISO (Multiple-Input Single-Output) system, i.e. $N = 1$ Rx antenna, while Figs. 4 and 5 compare them in a MIMO system with $N = 2$ Rx antennas. From the figures, we have the following two observations.

Firstly, although only partial diversity can be achieved, the QOSTFCs might still provide significantly better error performance, compared to the respective OSTFCs of the same order, while they are superior to the conventional

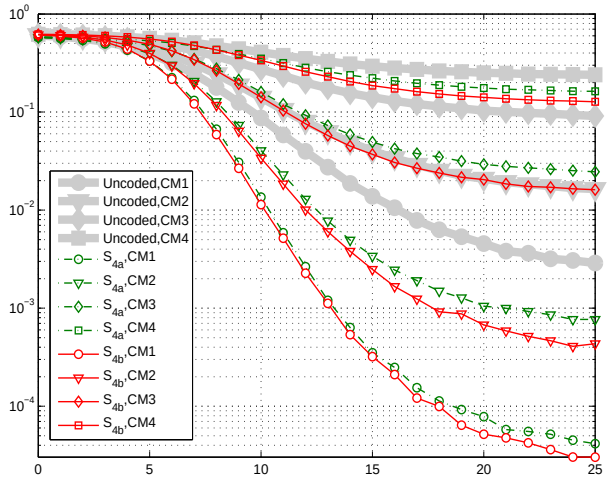

Fig. 2. S_{4b} vs. S_{4a} with 1 Rx antennas at the bit rate 480 Mbps.

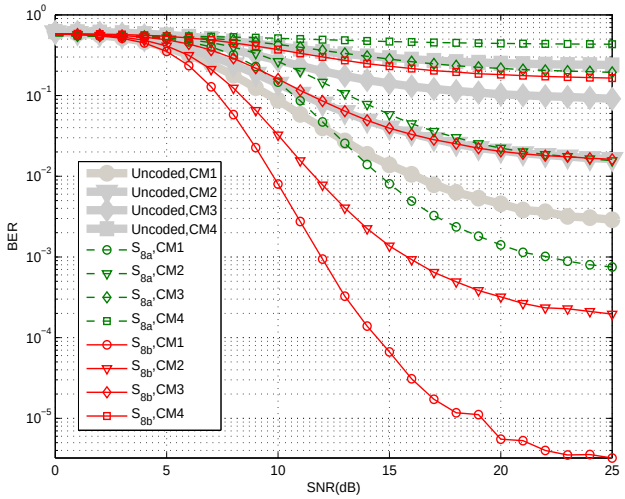

Fig. 3. S_{8b} vs. S_{8a}, with 1 Rx antennas at the bit rate 480 Mbps.

MB-OFDM. For example, from Figs. 4 and 5, we can see that QOSTFCs can provide better error performance of at least 1.2 dB for $\mathbf{S}_{4b}$ and 10 dB for $\mathbf{S}_{8b}$ at the bit error rate $BER = 10^{-5}$ in the case of $N = 2$, compared to their counterparts $\mathbf{S}_{4a}$ and $\mathbf{S}_{8a}$. The more dispersive the UWB channel model is (the dispersion increases from CM1 to CM4), the higher the gain is. We note that this enhancement is achieved without any increase of the total transmission power. Equivalently, the QOSTFCs may provide higher data rate with the same error performance as the OSTFCs.

Secondly, $\mathbf{S}_{8b}$ not only can provide higher system capacity (because of higher order as analyzed in Section 1), compared to $\mathbf{S}_{4b}$, but also might provide better error performance than $\mathbf{S}_{4b}$ (in the case of MISO systems - see Figs. 2 and 3) in the channel models CM1 and CM2 at the same data rate, while providing almost as good error performance as $\mathbf{S}_{4b}$ (in the case of MI2O systems - see Figs. 4 and 5). In

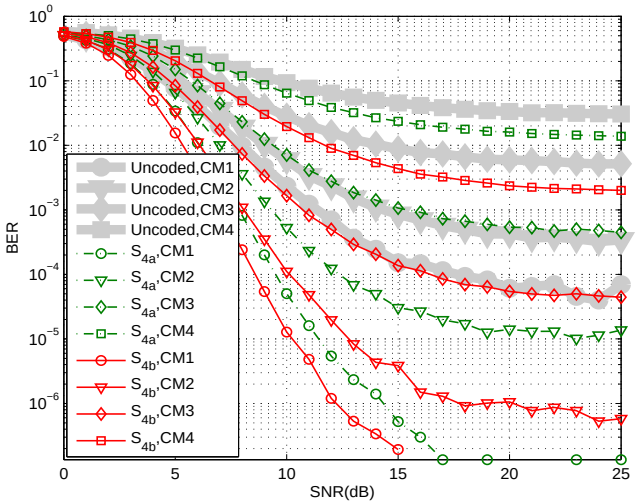

Fig. 4. S_{4b} vs. S_{4a} with 2 Rx antennas at the bit rate 480 Mbps.

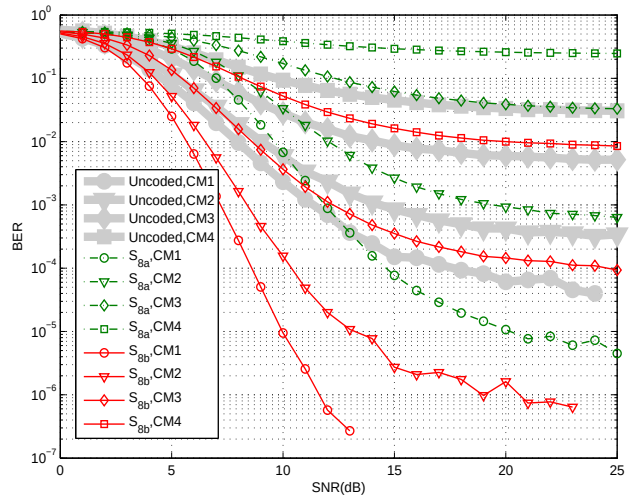

Fig. 5. S_{8b} vs. S_{8a}, with 2 Rx antennas at the bit rate 480 Mbps.

the more dispersive channel models CM3 and CM4, there exits a compromise between the system capacity and the code rate. The same applies to the error performance *if we compare the two codes at the same data rate*, since the decrease of the code rate of $\mathbf{S}_{8b}$, compared to that of $\mathbf{S}_{4b}$, causes the degradation of the error performance.

5. Conclusions

We have analyzed the application of QOSTFCs in our proposed STFC MB-OFDM UWB systems. Although only partial diversity can be achieved, QOSTFCs may still provide either a higher date rate or better error performance, compared to the full diversity OSTFC of the same order. Thus, it can be concluded that, for STFC MB-OFDM UWB, QOSTFCs might be better than OSTFCs, with the penalty of higher decoding complexity, though both have relatively simple decoding complexity. Furthermore, beside the case study of STFC MB-OFDM, it is our conjecture that the proposed QOSTFCs can also be used in various other wireless applications, such as WiMax MIMO [14], providing better BER than the respective OSTFCs. Examination of the application of OSTFCs and QOSTFCs in WiMax MIMO will be our future work.

Acknowledgment

L. C. Tran would like to thank the Alexander von Humboldt (AvH) Foundation, Germany, for its support of this work under the postdoctoral research fellowship. The authors are also grateful to the three anonymous reviewers for insightful comments.

References

[1] A. Batra et al., Multiband OFDM physical layer specification., WiMedia Alliance Release 1.1.

[2] I. E. Telatar, Capacity of multi-antenna Gaussian channels, European Trans. Telecom. 10 (6) (1999) 585–595.

[3] S. M. Alamouti, A simple transmit diversity technique for wireless communications, IEEE J. Select. Areas Commun. 16 (8) (1998) 1451 – 1458.

[4] V. Tarokh, N. Seshadri, A. R. Calderbank, Space-time codes for high data wireless communications: performance criterion and code construction, IEEE Trans. Inform. Theory 44 (2) (1998) 744 – 765.

[5] T.-H. Tan, K.-C. Lin, Performance of space-time block coded MB-OFDM UWB systems, Proc. 4th Annual Communication Networks and Services Research Conference (CNSR'06) (2006) 323 – 327.

[6] W. P. Siriwongpairat, W. Su, M. Olfat, K. J. R. Liu, Multiband-OFDM MIMO coding framework for UWB communication systems, IEEE Trans. Sign. Process. 54 (1) (2006) 214 – 224.

[7] L. C. Tran, A. Mertins, Space-time frequency code implementation in MB-OFDM UWB communications: design criteria and performance, accepted for publication in IEEE Trans. Wireless Commun. Available at http://www.isip.uni-luebeck.de/index.php?id=278.

[8] L. C. Tran, A. Mertins, E. Dutkiewicz, X. Huang, Space-time-frequency codes in MB-OFDM UWB communications: Advanced order-8 STFC and its performance, Proc. 7th IEEE International Symposium on Communications and Information Technologies ISCIT 2007.

[9] J. Foerster, I. R&D, Channel modelling sub-committee report final, IEEE P802.15 Working Group for Wireless Personal Area Networks (WPANs), IEEE P802.15-02/490r1-SG3a.

[10] L. C. Tran, A. Mertins, T. A. Wysocki, Quasi-orthogonal space-time-frequency codes in MB-OFDM UWB communications, Proc. International Conference on Signal Processing and Communication Systems ICSPCS2007.

[11] H. Jafarkhani, A quasi-orthogonal space-time block codes, IEEE Trans. Commun. 49 (1) (2001) 1 – 4.

[12] L. C. Tran, T. A. Wysocki, A. Mertins, J. Seberry, Complex Orthogonal Space-Time Processing in Wireless Communications, Springer, New York, USA, 2006.

[13] O. Tirkkonen, A. Hottinen, Square-matrix embeddable space-time blocks codes for complex signal constellations, IEEE Trans. Inform. Theory 48 (2) (2002) 384 – 395.

[14] R. B. Marks et al., IEEE tandard for local and metropolitan area networks. Part 16: Air interface for fixed and mobile broadband wireless access systems, IEEE 802.16e-2005.